Catalytic performance of $B_2O_3/TiO_2–ZrO_2$ for vapor-phase Beckmann rearrangement of cyclohexanone oxime: the effect of boria loading

Dongsen Mao [a,b,*], Guanzhong Lu [a], Qingling Chen [a,b], Zaiku Xie [b] and Yuxian Zhang [b]
[a] *Research Institute of Industrial Catalysis, East China University of Science and Technology, Shanghai 200237, PR China*
E-mail: maods@sript.com.cn
[b] *Shanghai Research Institute of Petrochemical Technology, Shanghai 201208, PR China*

Received 9 April 2001; accepted 10 August 2001

A series of boria catalysts supported on titania–zirconia mixed oxide ($B_2O_3/TiO_2–ZrO_2$) with different boria loadings (8–20 wt%) were prepared and characterized by X-ray diffraction, adsorption of nitrogen, ^{11}B magic angle spinning (MAS) NMR measurements and temperature-programmed desorption (TPD) of ammonia. The catalytic performance of $B_2O_3/TiO_2–ZrO_2$ for vapor-phase Beckmann rearrangement of cyclohexanone oxime to ε-caprolactam was studied at 300 °C. It was found that the lactam selectivity increased with increasing of boria loading, whereas a maximum oxime conversion was obtained at the boria loading of 12 wt%. The acid sites of medium strength on the surface of the catalyst play an important role in the selective formation of lactam.

KEY WORDS: Beckmann rearrangement; cyclohexanone oxime; ε-caprolactam; titanium–zirconium binary oxide; boria; $B_2O_3/TiO_2–ZrO_2$; acid catalyst

1. Introduction

There are numerous studies to rearrange the cyclohexanone oxime to ε-caprolactam (precursor to Nylon-6) over solid acid catalysts. Compared with the conventional method of preparing ε-caprolactam, this is an energetically and economically favorable as well as environmentally friendly alternative route, *e.g.*, there is no inevitable salt formation of ammonium sulfate. Among the solid acid catalysts studied, boria supported on an amorphous oxide has been mostly used. All of the oxide supports used are single metal oxides, such as alumina [1–3], silica [4,5], thoria [6], titania [7], zirconia [8–11], *etc*. In comparison with the single component supports, the composite oxide supports are found to exhibit higher surface acidity, surface area, thermal and mechanical strength [12]. Among various mixed oxides, the titania–zirconia binary oxide has been reported to exhibit high surface acidity by a charge imbalance based on the generation of Ti–O–Zr bonding [13]. Further, recent studies have revealed that $TiO_2–ZrO_2$ is an active catalyst for dehydrocyclization of *n*-paraffins to aromatics [14] and hydrogenation of carboxylic acids to alcohols [15], and also is an effective support for Ni-based catalyst for the hydrogenation of benzene [16]. Thus, the combined $TiO_2–ZrO_2$ oxide has attracted much attention recently as a catalyst and support for various applications.

In this paper, vapor-phase Beckmann rearrangement of cyclohexanone oxime to ε-caprolactam over titania–zirconia-supported boria catalysts is reported for the first time. The effect of boria loading on the structure, surface acidity and catalytic performance of $B_2O_3/TiO_2–ZrO_2$ was investigated in detail. The boria structures and acidities of the catalysts with different boria loadings were characterized by ^{11}B MAS NMR measurement and TPD of ammonia, respectively, in correlation with their catalytic performance for the Beckmann rearrangement reaction.

2. Experimental

2.1. Catalyst preparation

$TiO_2–ZrO_2$ binary oxide with a molar ratio of unity was prepared by coprecipitation in an aqueous solution containing titanium tetrachloride and zirconium oxychloride using aqueous ammonia as precipitation reagent. The precipitate was allowed to stand at room temperature for 24 h, filtered, washed with deionized water until no chloride ions were detected by adding $AgNO_3$ solution to the filtrate, and then dried at 110 °C for 24 h. After the powder of the dried precipitate was compressed into small dies, they were crushed and sieved to 40–60 mesh and calcined at 500 °C in air for 6 h.

Boria-supported catalysts with various boria loadings were prepared by multi-step pore-volume impregnation of $TiO_2–ZrO_2$ with an aqueous solution of boric acid. Between two impregnation steps the catalyst should be dried at 110 °C for at least 3 h. Finally, the catalyst was dried at 110 °C overnight and calcined at 600 °C for 12 h in air. Boria loading was changed from 8 to 20 wt% as B_2O_3.

---

[*] To whom correspondence should be addressed.

1011-372X/01/1100-0119$19.50/0

For comparison purpose, supported boria catalysts (with boria loading of 12 wt%) on the single component oxides TiO_2 and ZrO_2 and on other binary oxides including SiO_2–Al_2O_3, SiO_2–TiO_2, SiO_2–ZrO_2, Al_2O_3–TiO_2 and Al_2O_3–ZrO_2 were similarly prepared.

2.2. Catalyst characterization

The crystal structure was identified by XRD (Rigaku D/MAX-1400) measurements using Cu Kα radiation at 40 kV and 40 mA.

BET surface areas, pore volume and pore size distributions of the $B_2O_3/TiO_2–ZrO_2$ catalysts were measured on a Micromeritics Digisorb 2600 system under liquid-N_2 temperature using N_2 as the adsorbate. Samples were outgassed under vacuum at 450 °C for 3 h immediately prior to analysis.

^{11}B (8 ° rf pulses, 1 s recycle delay) MAS NMR spectra were recorded at resonance frequency of 96.29 MHz on a Bruker DMX-300 multinuclear spectrometer, while a MAS spinner was rotated at a rate of 12 kHz. Background subtraction was necessary due to boron nitride components in the probe. Chemical shifts reported in parts per million (ppm) were referenced to BF_3 etherate.

NH_3-TPD experiments were conducted in a conventional flow apparatus equipped with a thermal conductivity detector. The sample (100 mg) was pretreated under a helium stream flow (30 ml/min) at 500 °C for 1 h and then flushed with a mixture of NH_3 (9.84 vol%)–He for 0.5 h at 150 °C. Subsequently, the sample was outgassed at the same temperature for 1 h in helium stream to remove physisorbed ammonia. The TPD of NH_3 was measured from 150 to 550 °C at a heating rate of 10 °C/min.

2.3. Rearrangement of cyclohexanone oxime

The catalytic rearrangement of oxime was performed under atmospheric pressure using a continuous-flow fixed-bed reactor (6 mm i.d.) made of stainless steel. The feed (5 wt% cyclohexanone oxime in benzene) was injected to the reactor by a syringe pump (Gilson S.A.) at 6 ml/h with nitrogen carrier gas flowing at 30 ml/min. The reaction conditions were as follows: 0.8 g of catalyst, reaction temperature of 300 °C, 0.1 MPa and WHSV of 0.33 $g_{oxime}/g_{cat}^{-1}\,h^{-1}$. The reactor effluent was collected by a glass trap which was immersed in an ice-water bath. The products collected were analyzed by a gas chromatograph (Hewlett–Packard 4890D) equipped with a capillary column (HP-1) and a FID detector. The used catalyst was regenerated by calcination *in situ* in dry air at 600 °C for 8 h.

3. Results

3.1. Catalyst characterization

XRD patterns of the $TiO_2–ZrO_2$ support calcined at various temperatures from 500 to 1000 °C are shown in figure 1. After calcining at 500 °C, the $TiO_2–ZrO_2$ mixed support was in an amorphous state. However, sharp X-ray diffraction lines characteristic of the formation of the crystalline $ZrTiO_4$ compound ($2\theta = 24.7°$ and $30.6°$) can be observed from 650 °C and above temperatures, and the intensity of lines due to this compound also increased with increase in calcination temperature. A similar observation was also made earlier by Fung *et al.* [14]. Moreover, no independent diffraction peaks assigned to TiO_2 (anatase or rutile) or ZrO_2 (monoclinic, tetragonal or cubic) phases were detected in the XRD patterns of $TiO_2–ZrO_2$. The $ZrTiO_4$ compound appears to be thermally quite stable even up to 1000 °C calcination temperature (figure 1). The higher thermal stability of the support is advantageous since it allows the regeneration of deactivated catalysts by high temperature calcination.

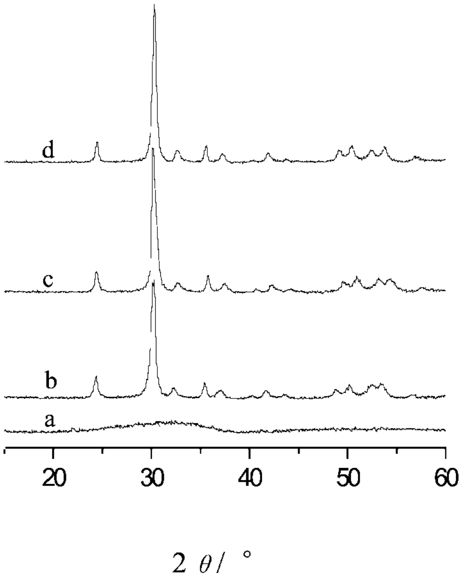

Figure 1. XRD patterns of $TiO_2–ZrO_2$ support calcined at various temperatures: (a) 500, (b) 650, (c) 800 and (d) 1000 °C.

The X-ray diffractograms of $B_2O_3/TiO_2–ZrO_2$ catalysts with various boria loadings are depicted in figure 2. As can be seen from this figure, the $B_2O_3/TiO_2–ZrO_2$ catalysts showed sharp diffraction lines indicating the formation of $ZrTiO_4$ compound. The intensity of these bands increased with boria loading. This result indicated that the transformation of amorphous $TiO_2–ZrO_2$ mixed oxide into a crystalline $ZrTiO_4$ compound is accelerated by the supported boria. This similar phenomenon was also observed by Bautista *et al.* [17] for the boria catalysts supported on Al_2O_3 and $AlPO_4$ carriers. In addition, as shown in figure 2, the characteristic peak of crystalline B_2O_3 ($2\theta = 28°$) was observed in the XRD patterns of all the $B_2O_3/TiO_2–ZrO_2$ catalysts, and the intensity of the diffraction line was almost the same regardless of the boria loading. This observation was in contrast with that reported for the B_2O_3/Al_2O_3 catalysts [18], in which the intensity of the diffraction line due to crystalline B_2O_3 increased with the boria loading. From the result above, it is clear that most of the boria supported on $TiO_2–ZrO_2$ mixed oxide existed in its vitreous state.

The BET surface areas of the $B_2O_3/TiO_2–ZrO_2$ catalysts were measured together with that of the support calcined

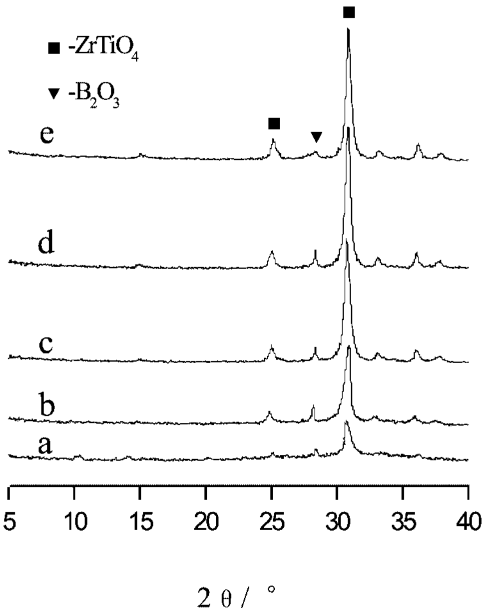

Figure 2. XRD patterns of B_2O_3/TiO_2–ZrO_2 catalysts with various boria loadings: (a) 8, (b) 10, (c) 12 , (d) 15 and (e) 20 wt%.

Table 1
BET surface area of various samples calcined at 600 °C.

Sample	S_{BET} (m^2/g_{cat})	S_{BET} ($m^2/g_{support}$)
TiO_2–ZrO_2	103.0	103.0
8% B_2O_3/TiO_2–ZrO_2	45.9	49.9
10% B_2O_3/TiO_2–ZrO_2	39.1	43.4
12% B_2O_3/TiO_2–ZrO_2	17.6	20.0
15% B_2O_3/TiO_2–ZrO_2	14.7	17.3
20% B_2O_3/TiO_2–ZrO_2	9.0	11.2

at 600 °C. The results are summarized in table 1. The surface area of the TiO_2–ZrO_2 support was about 103 m^2/g, but it decreased monotonously with increasing B_2O_3 loading. Table 1 also presents the BET surface areas expressed per gram of support. These data suggest that modification of the TiO_2–ZrO_2 occurred due to pore filling by B_2O_3 in addition to the relative decrease in support content of the catalyst.

The pore size distribution of B_2O_3/TiO_2–ZrO_2 was measured to study the process of B_2O_3 deposition on the internal surface of TiO_2–ZrO_2. The results are illustrated in figure 3. As shown, the TiO_2–ZrO_2 support after calcination at 600 °C had a sharp peak at 5.6 nm in the pore size distribution. After the loading of boria (8 wt%), the small pores of the TiO_2–ZrO_2 decreased and a broad peak at between 15 and 70 nm appeared simultaneously. Engels *et al.* [19] also observed that new pores with diameter larger than 50 nm appeared after supporting B_2O_3 on Al_2O_3. As the boria loading increased, the small pore disappeared and the centered pore size of the broad peak shifted to high value (figure 3). At the same time, the pore volume decreased from 0.272 to 0.055 cm^3/g.

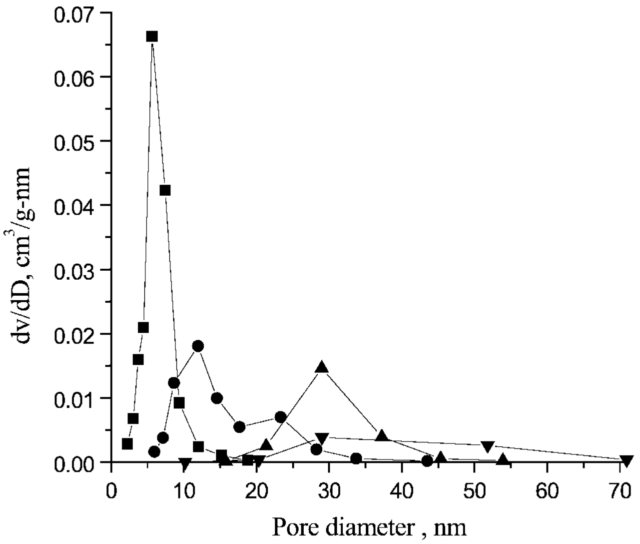

Figure 3. Pore size distributions of various samples calcined at 600 °C: (■) TiO_2–ZrO_2, (•) 8% B_2O_3/TiO_2–ZrO_2, (▲) 12% B_2O_3/TiO_2–ZrO_2 and (▼) 15% B_2O_3/TiO_2–ZrO_2.

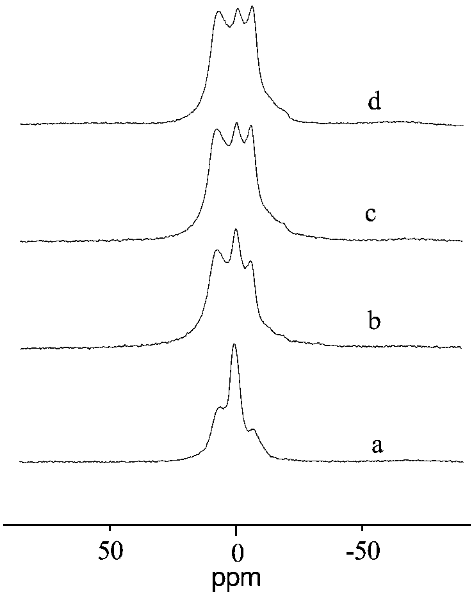

Figure 4. ^{11}B MAS NMR spectra of B_2O_3/TiO_2–ZrO_2 catalysts with different boria loading: (a) 8, (b) 12, (c) 15 and (d) 20 wt%.

In amorphous and crystalline compounds boron may exist in tetrahedral BO_4 units and trigonal BO_3 units [20,21]. Figure 4 displays the ^{11}B MAS NMR spectra of B_2O_3/TiO_2–ZrO_2 catalysts with different boria loadings. The BO_4 signal gave a sharp resonance peak at *ca.* 2 ppm. The signal for trigonally coordinated BO_3 was split and broadened due to a second-order quadrupolar effect. This doublet however, corresponds to a single signal [22]. Unfortunately, the field strength used here (300 MHz) resulted in an overlap of the trigonal and tetrahedral signals. Despite this overlap, the trigonal and tetrahedral signals can be easily seen in the spectra and integrated. As shown in figure 4, all the samples consisted of both trigonal and tetrahedral B–O coordinations. With an increase in boria loading, the intensity of tetrahedral signal decreased but that of trigonal signal increased. Thus, the ratio of BO_3 to BO_4 species increased with increasing boria loading.

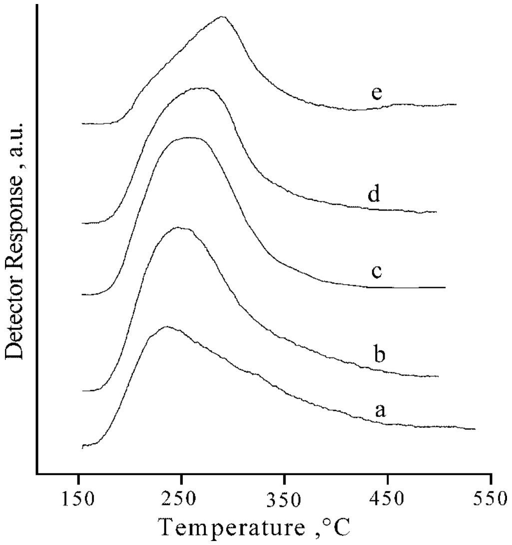

Figure 5. NH_3-TPD profiles of $B_2O_3/TiO_2–ZrO_2$ catalysts with different boria loadings: (a) 8, (b) 10, (c) 12, 15 and (e) 20 wt%.

Acidic properties were investigated using the adsorption of probe molecules by TPD. The TPD profiles of the ammonia adsorbed on the $B_2O_3/TiO_2–ZrO_2$ catalysts with different boria loadings are depicted in figure 5. The TPD profiles show that the acid strength of the catalysts increased with boria loading, which was indicated by a continuous shift of the desorption peak of maximum height to higher desorption temperatures. However, the total desorbed ammonia or total area of the TPD peaks decreased with increase of boria loading, indicating a decrease in the total number of acid sites calculated per unit mass of catalyst.

3.2. Rearrangement reaction

The supported boria catalysts were tested for the Beckmann rearrangement of cyclohexanone oxime to ε-caprolactam at 300 °C. The by-products of this reaction were mainly cyclohexanone, 2-cyclohexenone, cyanopentane, 5-cyano-1-pentene and aniline. The conversion of oxime decreased with time on stream, while the selectivity to lactam kept the initial value for the first 10 h on stream, and this was a general finding for all catalysts tested. The conversion of cyclohexanone oxime and the selectivity and yield to ε-caprolactam over the supported boria catalysts after 2 h on stream are presented in table 2. The data show that $B_2O_3/TiO_2–ZrO_2$ was by far the best catalyst tested for this reaction in terms of selectivity and yield of lactam.

Table 2
Performance of various supported boria catalysts for Beckmann rearrangement of cyclohexanone oxime.[a]

Catalyst[b]	Conversion (%)	Selectivity (%)	Yield (%)
$B_2O_3/TiO_2–ZrO_2$	100	97.4	97.4
B_2O_3/TiO_2	100	83.8	83.8
B_2O_3/ZrO_2	100	79.3	79.3
$B_2O_3/SiO_2–Al_2O_3$	100	60.0	60.0
$B_2O_3/SiO_2–TiO_2$	17.5	35.1	6.14
$B_2O_3/SiO_2–ZrO_2$	22.6	31.1	7.03
$B_2O_3/Al_2O_3–TiO_2$	97.4	36.2	35.2
$B_2O_3/Al_2O_3–ZrO_2$	35.2	40.0	14.1

[a] Reaction conditions: $T = 300\,°C$, $P = 0.1$ MPa; WHSV $= 0.33\,h^{-1}$ and time on stream 2 h.
[b] Boria loading 12 wt%.

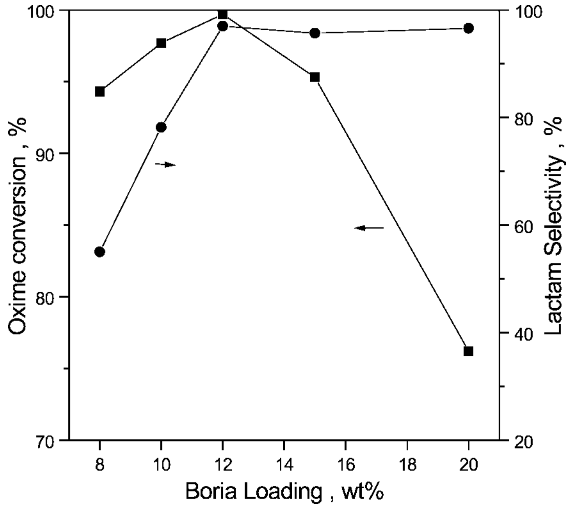

Figure 6. Effect of boria loading on the oxime conversion and lactam selectivity over $B_2O_3/TiO_2–ZrO_2$ catalysts (data were averaged for 5 h on stream).

The performance of $B_2O_3/TiO_2–ZrO_2$ catalysts with various boria loadings was examined at 300 °C. Figure 6 shows the average oxime conversion and the average lactam selectivity during the first 5 h of the reaction. Apparently, the boria loading affects remarkably the activity and selectivity of $B_2O_3/TiO_2–ZrO_2$ catalysts. The oxime conversion increased with boria loading up to 12 wt% and then decreased as the loading of boria is further increased. Surprisingly, the lactam selectivity also increased with increasing boria loading to 12 wt% as the same loading of the maximum oxime conversion; above this loading the selectivity to lactam changed hardly.

The regeneration ability of a catalyst is very important in the practical use in industry. As illustrated in figure 7, the $B_2O_3/TiO_2–ZrO_2$ catalyst with boria loading of 12 wt% had excellent regeneration ability. After a regeneration process of heating the used catalyst *in situ* in dry air at 600 °C for 8 h, the activity of the regenerated catalyst was almost identical with that of the fresh catalyst. Two main mechanisms have been suggested for the deactivation of solid acid catalysts in the rearrangement reaction of oxime: the formation of coke [1,3,23] and/or the irreversible adsorption of basic reaction by-products [24]. Since the deactivated catalyst can be completely regenerated by burning off the coke in air, we feel confident to propose that coke formation was the main reason for the deactivation.

4. Discussion

Catalytic results show a clear dependence of the activity data on the boria loading. It is well known that two boron

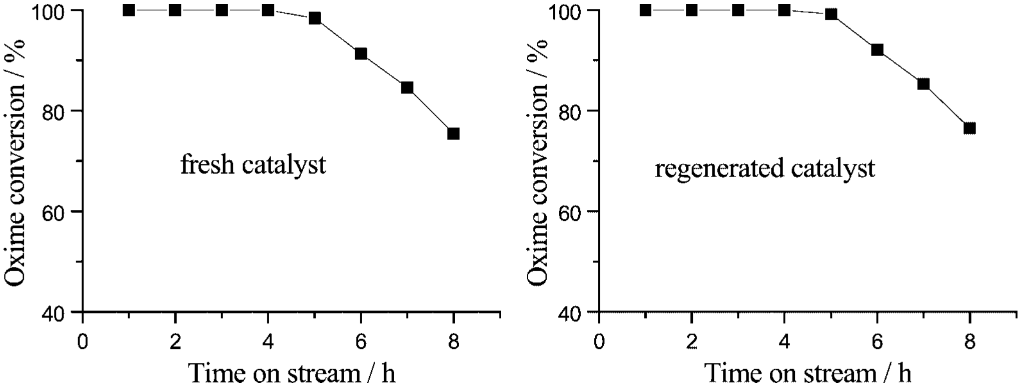

Figure 7. Regeneration ability of 12% $B_2O_3/TiO_2–ZrO_2$ catalyst.

species can be present on the support and the nature and their relative ratio depend on preparation method, calcination temperature, boria loading, *etc*. The characterization of the $B_2O_3/TiO_2–ZrO_2$ catalysts by ^{11}B MAS NMR and NH_3-TPD, reveals that boria loading determines the nature of the supported species as well as their acidic properties.

On the basis of the ^{11}B MAS NMR measurements, it is apparent that both trigonal and tetrahedral coordinated borons were present in all the $B_2O_3/TiO_2–ZrO_2$ catalysts. The relative amounts of the two coordinations were dependent on the boria loading and the ratio of BO_3 to BO_4 species increased with increase of boria loading. This is more evident from figure 8 comparing the integrated signals in terms of BO_3/BO_4 ratio. The results of figure 8 show a trend rather than an absolute ratio of BO_3/BO_4, because the intensity of the tetrahedral signal is higher than that of an equivalent amount of trigonal boron. This intensity difference arises from combined effects of the difference in the quadrupolar coupling constants of two coordinations and 8° pulse angle used [22].

As seen from the NH_3-TPD studies, the boria loading of $B_2O_3/TiO_2–ZrO_2$ catalyst affects markedly their acidity. The variation in concentration of acid sites (per m^2 catalyst), which was calculated by dividing the total integrated area of the NH_3 band by the BET surface area of the sample, with the boria loading was also presented in figure 8, which indicates the same trend as the ratio of BO_3/BO_4, increasing acid site concentration with increase of boria loading. From figure 8, it is clear there is a direct relationship between the concentration of acid sites on the surface of $B_2O_3/TiO_2–ZrO_2$ catalysts and the particular coordination of the boron atom. It is the trigonal coordinated boron that is responsible for the enhanced acidity observed. This observation was in contrast with that reported for the B_2O_3/Al_2O_3 catalysts [22], in which both the strength and concentration of acid sites increased as the relative amounts of tetrahedral boron increased.

The relationship between acidic properties and catalytic performance has been studied by many researchers. It has been reported that a relative strong acid site ($H_0 < -5.6$) of B_2O_3/SiO_2 is responsible for the formation of ε-caprolactam [5]. On the other hand, Takahashi *et al.* reported for the H-ZSM-5 zeolite modified by B_2O_3 that lactam selectivity improves with the increase of the ratio of weak acid sites to strong acid sites [25]. Curtin *et al.* demonstrated that the lactam selectivity is directly proportional to the concentration of medium strength acid sites on the B_2O_3/Al_2O_3 catalysts from which ammonia desorbed between 200 and 350 °C [3,23,26,27]. Xu *et al.* reported that the active sites for Beckmann rearrangement are the medium and strong acid sites on the surface of B_2O_3/ZrO_2 catalysts, which were characterized by desorption of adsorbed ammonia >200 °C [9].

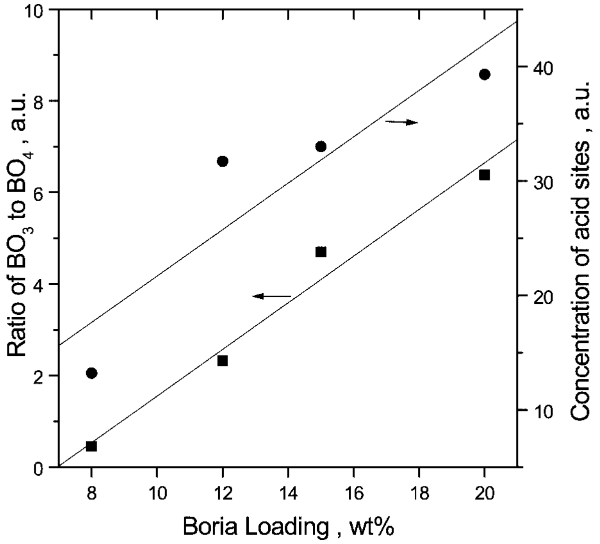

Figure 8. Relationship between boron–oxygen coordination of $B_2O_3/TiO_2–ZrO_2$ catalysts with different boria loadings and their concentration of acid sites.

In the present work, as the boria loading increased, the total concentration of acid sites on $B_2O_3/TiO_2–ZrO_2$ catalysts increased (figure 8), while the total number of acid sites decreased (figure 5) because the surface area decreased monotonously (table 1). However, catalytic results revealed that a maximum oxime conversion was obtained at the boria loading of 12 wt% and the lactam selectivity saturated when the boria loading was more than 12 wt%. Such results suggested that the activity and selectivity of $B_2O_3/TiO_2–ZrO_2$ catalyst were dependent on their acid strength distributions.

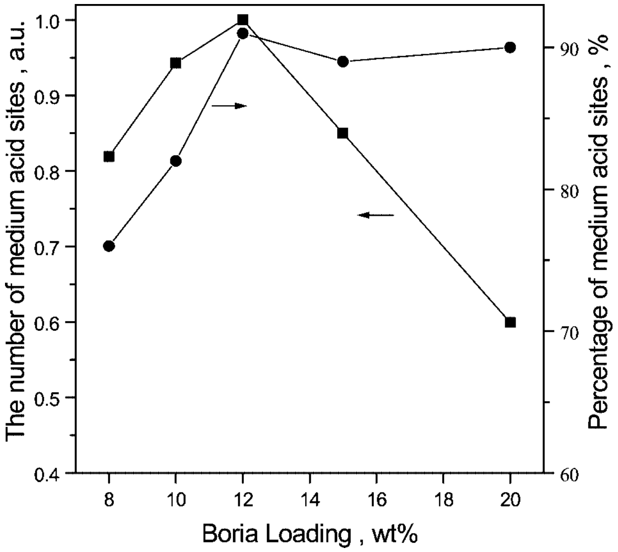

Figure 9. Plots of acidity of $B_2O_3/TiO_2–ZrO_2$ catalysts *vs*. boria loading.

The acid strength distributions were obtained by analyzing the TPD curves of adsorbed ammonia following the procedure proposed by Berteau and Delmon [28]. The number of weak, medium and strong acid sites were related to the number of NH_3 molecules desorbed up to 200 °C, between 200 and 350 °C, and above 350 °C, respectively. The acidity distributions of catalysts were expressed as the integrated area of the NH_3 band developed in a given range of temperature. The total integrated area of the NH_3 band was considered as a measure of total number of acid sites. In figure 9, the number of medium strength acid sites and its percentage to the total number of acid sites were plotted against the boria loading. Although the total number of acid sites over $B_2O_3/TiO_2–ZrO_2$ catalysts decreased with boria loading, the percentage of the medium strength acid sites increased; as a result, the number of medium strength acid sites presented a maximum at 12 wt% boria loading (figure 9). Comparison of figures 6 and 9 shows clearly that the catalytic activity of $B_2O_3/TiO_2–ZrO_2$ catalyst is in parallel with the number of medium strength acid sites. The highest oxime conversion was obtained over 12 wt% $B_2O_3/TiO_2–ZrO_2$ catalyst which contained the maximum number of medium strength acid sites. On the other hand, the selectivity to lactam is in good agreement with the desorption percentage. On the basis of these results, we concluded that the acid sites of medium strength are effective for the selective formation of lactam.

5. Conclusions

The acidic and catalytic properties of boria supported on $TiO_2–ZrO_2$ binary oxide for vapor-phase Beckmann rearrangement of cyclohexanone oxime were found to be affected by the boria loading. It was suggested that the medium strength acid sites, which were characterized by desorption of adsorbed ammonia between 200 and 350 °C, are responsible for the selective formation of ε-caprolactam. As the boria loading increased, the strength and concentration of acid sites of $B_2O_3/TiO_2–ZrO_2$ catalysts increased, but the surface area decreased. Optimum boria loading was at 12 wt%, which contained the maximum number of medium strength acid sites. It was the trigonal coordinated boron species that is responsible for the enhanced acidity observed.

Acknowledgement

We gratefully acknowledge the financial support from Shanghai Research Institute of Petrochemical Technology.

References

[1] S. Sato, S. Hasebe, H. Sakurai, K. Urabe and Y. Izumi, Appl. Catal. A 29 (1987) 107.
[2] H. Sakurai, S. Sato, K. Urabe and Y. Izumi, Chem. Lett. (1985) 1783.
[3] T. Curtin, J.B. McMonagle and B.K. Hodnett, Appl. Catal. A 93 (1992) 91.
[4] S. Sato, H. Sakurai, K. Urabe and Y. Izumi, Chem. Lett. (1985) 277.
[5] S. Sato, K. Urabe and Y. Izumi, J. Catal. 102 (1986) 99.
[6] W.F. Yates, R.O. Downs and J.C. Burleson, US Patent 3639391 (1972).
[7] K. Yoshida, K. Fujiki, T. Harada, Y. Moroi and T. Yamaguchi, Jpn. Patent 7310478 (1973).
[8] S.B. Cheng, B.Q. Xu, S. Jiang, F.P. Tian, T.X. Cai and X.S. Wang, Chin. J. Catal. 17 (1996) 512.
[9] B.Q. Xu, S.B. Cheng, S. Jiang and Q.M. Zhu, Appl. Catal. A 188 (1999) 361.
[10] B.Q. Xu, S.B. Cheng, X. Zhang, S.F. Ying and Q.M. Zhu, Chem. Commun. (2000) 1121.
[11] B.Q. Xu, S.B. Cheng, X. Zhang and Q.M. Zhu, Catal. Today 63 (2000) 275.
[12] J.B. Miller, S. Rankin and E.I. Ko, J. Catal. 148 (1994) 673.
[13] J.C. Wu, C.S. Chung, C.L. Ay and I. Wang, J. Catal. 87 (1984) 98.
[14] J. Fung and I. Wang, J. Catal. 130 (1991) 577.
[15] K. Takahashi, M. Shibagaki and H. Matsushita, US Patent 5576467 (1996).
[16] I. Wang, W.H. Huang and J.C. Wu, Appl. Catal. 18 (1985) 273.
[17] F.M. Bautista, J.M. Campelo, A. Garcia, D. Luna, J.M. Marinas, M.C. Moreno, A.A. Romero, J.A. Navio and M. Macias, J. Catal. 173 (1998) 333
[18] Y. Murakami, K. Otsuka, Y. Wada and A. Morikawa, Bull. Chem. Soc. Jpn. 63 (1990) 340
[19] S. Engels, E. Herold, H. Lausch, H. Mayr, H.W. Meiners and M. Wilde, Stud. Surf. Sci. Catal. 75 (1993) 2581.
[20] G.L. Turner, K.A. Smith, R.J. Kirkpatrick and E. Oldfield, J. Magn. Reson. 67 (1986) 544.
[21] S. Sato, M. Kuroki, T. Sodesawa, F. Nozaki and G.E. Maciel, J. Mol. Catal. A 104 (1995) 171.
[22] K.P. Peil, L.G. Galya and G. Marcelin, J. Catal. 115 (1989) 441.
[23] T. Curtin, J.B. McMonagle and B.K. Hodnett, Appl. Catal. A 93 (1992) 75.
[24] A. Aucejo, M.C. Burguet, A. Corma and V. Fornes, Appl. Catal. 22 (1986) 187.
[25] T. Takahashi, K. Ueno and T. Kai, Canad. J. Chem. Eng. 69 (1991) 1096.
[26] T. Curtin, J.B. McMonagle and B.K. Hodnett, Catal. Lett. 17 (1993) 145.
[27] T. Curtin, J.B. McMonagle and B.K. Hodnett, Stud. Surf. Sci. Catal. 75 (1993) 2609.
[28] P. Berteau and B. Delmon, Catal. Today 5 (1989) 121.